Alumina Supported Cu-Mn-La Catalysts for CO and VOCs Oxidation

Elitsa N. Kolentsova, Dimitar Y. Dimitrov, Petya Cv. Petrova, Georgi V. Avdeev, Diana D. Nihtianova, Krasimir I. Ivanov, Tatyana T. Tabakova

Abstract—Recently, copper and manganese-containing systems are recognized as active and selective catalysts in many oxidation reactions. The main idea of this study is to obtain more information about γ-Al₂O₃ supported Cu-La catalysts and to evaluate their activity to simultaneous oxidation of CO, CH₃OH and dimethyl ether (DME). The catalysts were synthesized by impregnation of support with a mixed aqueous solution of nitrates of copper, manganese and lanthanum under different conditions. XRD, HRTEM/EDS, TPR and thermal analysis were performed to investigate catalysts' bulk and surface properties. The texture characteristics were determined by Quantachrome Instruments NOVA 1200e specific surface area and pore analyzer. The catalytic measurements of single compounds oxidation were carried out on continuous flow equipment with a fourchannel isothermal stainless steel reactor in a wide temperature range. On the basis of XRD analysis and HRTEM/EDS, it was concluded that the active component of the mixed Cu-Mn-La/y-alumina catalysts strongly depends on the Cu/Mn molar ratio and consisted of at least four compounds - CuO, La₂O₃, MnO₂ and Cu_{1.5}Mn_{1.5}O₄. A homogeneous distribution of the active component on the carrier surface was found. The chemical composition strongly influenced catalytic properties. This influence was quite variable with regards to

Keywords—Supported copper-manganese-lanthanum catalysts.

I. INTRODUCTION

T HE perovskites of the formula ABO₃ are widely used as catalysts in various reactions such as oxidation of CO and volatile organic compounds, reduction of nitrogen oxide and others [1]-[3]. On the one hand, these oxides offer the possibility for preparation of a large series of isomorphous solids solids at the partial replacement of A and B cations ($A_{L-x}A'_xB_{L-y}B'_yO_3$), which are very stable at high temperatures and can be used in many fields, such as catalytic combustion at high temperatures where other formulations are inapplicable. A disadvantage of these mixed oxides, however, is their small

Elitsa Kolentsova is with the Department of Chemistry, Agricultural University, 4000 Plovdiv, Bulgaria (corresponding author, phone: +359-887-745-734; fax: +359-32-633-157; e-mail: elitsa_kolentsova@abv.bg).

Dimitar Dimitrov and Krasimir Ivanov are with the Department of Chemistry, Agricultural University, 4000 Plovdiv, Bulgaria (e-mail: mitko_dme@abv.bg, kivanov1@ abv.bg).

Petya Petrova and Tatyana Tabakova are with the Institute of Catalysis, Bulgarian Academy of Science, 1113 Sofia, Bulgaria (e-mail: petya@ic.bas.bg, tabakova@ic.bas.bg).

Georgi Avdeev is with the Institute of Physical Chemistry, Bulgarian Academy of Science, 1113 Sofia, Bulgaria (e-mail: g_avdeev@ipc.bas.bg).

Diana Nihtianova is with the Institute of Mineralogy and Crystallography, Bulgarian Academy of Sciences, 1113 Sofia, Bulgaria (e-mail: diana.nihtianova@gmail.com)

specific surface area. In the scientific literature, there are many studies on preparation methods aimed at increasing the specific surface area of the monolithic mixed oxide [4] and accelerating of the synthesis, but in all cases, the specific surface is between 5 and 50 m²/g. Therefore, over the last decade, the efforts are directed to preparation of supported perovskites with large specific surface [5].

The preparation method can critically influence the morphology of the materials, affecting their catalytic activity. Various methods are known in the literature for synthesis of nanostructured metal oxide, most often co-precipitation, solgel, microemulsion methods, glycine-nitrate method, vapor condensation and others [6]. An alternative method for increasing the specific surface area of the perovskites is their impregnation on materials such as alumina or cordierite. A serious problem, however, is the opportunity for solid phase reactions between the components of the active phase and the carrier at high temperatures [7].

The study of the lanthanides for various catalytic processes is a subject of increasing interest over the past few decades [8]. Cerium oxide is often used in the oxidation of volatile organic compounds as carrier or as mixed oxides with other metals [6], but only a few studies in the scientific literature have reported the behavior of catalysts based on lanthanum oxide. Chen et al. have synthesised La-Co and La-Cu oxides by several methods - by use of carbon matrix (exotemplating), glycine-nitrate method (GN), and a mixed process (GNexotemplating) and have found that an increase in the temperature of ignition caused decrease of specific surface of the catalyst. In the diffractograms of the samples calcined at high temperatures (800°C), La₂CuO₄ and LaCoO₃ were detected; but the catalytic activity of these samples was low. Complete oxidation of ethyl acetate on La-Co samples was reached at lower temperatures as compared with samples, containing La-Cu. La-Co samples, synthesized by GN method (atomic ratio La-Co 1:1) and calcined at 600°C showed the highest catalytic activity for this reaction among all the lanthanum-containing samples. 100% conversion of ethyl acetate to H₂O and CO₂ was achieved at 230°C.

According to the authors, the catalytic activity was affected mainly by the amount and nature of the transition metal (Cu or Co) in the samples, temperature of calcination, presence of perovskite oxides and reducibility of the catalyst [6]. The aim of present work was to study the effect of chemical composition on the activity of γ -alumina supported CuO/MnO₂/La₂O₃ samples toward deep oxidation of CO, methanol and DME.

II. EXPERIMENTAL

A. Catalysts Preparation

For preparation of catalytic materials, wet impregnation method was applied. Commercial γ -alumina (fraction 0.6-1.0 mm) was used as a support after calcination for 2 hours at 450 °C. Mixed solution of copper, manganese and lanthanum nitrates with different composition was added to carrier at a room temperature. The impregnation was carried out 12 hours at 80 °C. The resulting materials were dried at 120 °C for 10 hours and calcined at 450 °C for 4 hours. The total amount of active phase was 20 wt. %.

B. Catalyst Characterization

• Thermal Analysis (TG, DTG and DTA)

Thermal analysis of the samples were performed in computerized thermal installation "Stanton Redcroft" (England) under the following experimental conditions: heating rate – 10 °C.min⁻¹, range of heating temperature - 20 to 650 °C sample mass - 12.00 mg in air and stabilized corundum pot.

• Texture Measurements

The texture characteristics were determined in a Quantachrome Instruments NOVA 1200e (USA) specific surface area & pore analyser by low-temperature (-195 °C) nitrogen adsorption.

• Powder X-ray Diffraction (XRD)

The phase composition was characterized by X-ray powder diffraction (XRD) using a PANalytical Empyrean equipped with a multichannel detector (Pixel 3D) using (Cu K_{α} 45 kV-40 mA) radiation in the 20–115° 2θ range, with a scan step of 0.01° for 20 s.

• Transmission Electron Microscopy (TEM)

Transmission electron microscopy (TEM) and high resolution TEM (HRTEM) were performed by a JEOL 2100 instrument at accelerating voltage 200 kV, equipped with a XEDS spectrometer (Oxford instruments, X-max^N 80T) and STEM module. Selected Area Electron Diffraction (SAED) was also employed to have information on the nature of the crystalline phases.

• Temperature Programmed Reduction (TPR)

TPR measurements were conducted in a flow system under the following conditions: Gas mixture hydrogen-argon (10% H_2); temperature rise 15 $^{\circ}\text{C.min}^{\text{-}1}$; flow rate 24 ml.min $^{\text{-}1}$ and sample amount of 0.05 g.

• Activity Measurements

Gas mixtures on the input and output of the reactor were analyzed with a gas chromatograph HP 5890 Series II, equipped with TCD and FID detectors, column Porapak Q (for CO₂, methanol and DME) and column MS-5A (for oxygen, nitrogen and CO).

The activity of the catalysts was rated according to the oxidation degree of the gases, passed through the catalyst layer, in percentages.

III. RESULTS

• Thermal Analysis (TG, DTG and DTA)

Fig. 1 shows TG, DTG and DTA curves of the lanthanum nitrate in a temperature range from room temperature to 700 °C. There are four well-defined areas of weight loss with total weight loss of 26.55% (64.18%, recalculated on the basis of the supported substance). This value is very close to the theoretical value of 62.36%, calculated according to the formulas of La(NO₃).6H₂O and La₂O₃. Obviously, the weight loss of 7.52% at temperature range to 220 °C is associated with the release of adsorbed and crystallization water. The weight losses in the second (220 to 365 °C - 8.25%), third (365 to 476 °C - 8.92%) and fourth (over 476 °C - 3.43%) stages show that decomposition of the supported lanthanum nitrate proceeds stepwise. This finding is consistent with the results of [9] according to which, decomposition of the lanthanum nitrate after removal of the crystallization water takes place in three stages with the formation of two intermediates with a composition LaONO3, La3O4NO3 and decomposition of the latter to La₂O₃. According to the same authors, complete decomposition of the lanthanum nitrate needs calcination of the sample at temperatures above 570 °C, which requires a treatment at high temperature of La₂O₃-based catalyst samples.

DTA, DTG and TGA analysis of the samples with an atomic ratio Cu/La 2:1 and of the mixed Cu-Mn-La catalysts, in which manganese is partially replaced by lanthanum, are presented in Figs. 2-4 and Table I.

The results presented in Fig. 2 show that the decomposition of lanthanum nitrate in the mixture $\text{Cu(NO}_3)_2$ - $\text{La(NO}_3)_3$ occurs by different mechanism and at significantly lower temperatures. Obviously, 12.1% weight reduction (53.3% of total weight loss) in the temperature range from 120 to 300 °C is mainly related to the decomposition of copper nitrate, while the loss of 9.1% (40.4% of total weight loss) at temperatures above 300 °C - to decomposition of the lanthanum nitrate.

 $TABLE\ I$ Thermogravimetric Results for Different Cu-Mn/ γ -Al $_2O_3$ Catalysts

	Weight loss			
Sample.	First	Second	Third	Forth
	Onset temp.,°C	Onset temp.,°C	Onset temp.,°C	Onset temp.,°C
	(Weight loss,%)	(Weight loss,%))	(Weight loss,%)	(Weight loss,%)
Fig. 1	45	220	365	476
	(7.5)	(8.5)	(8.9)	(3.4)
Fig. 2	42	121	300	-
	(2.0)	(12.1)	(9.1)	-
Fig. 3	47	138	-	-
	(2.4)	(16.6)	-	-
Fig. 4	47	156	282	-
	(2.4)	(16.6)	(7.6)	

The results of the thermal analysis of the mixed Cu-Mn-La/γ-Al₂O₃ catalyst confirmed the assumption for different mechanism of decomposition of the salts in the mixture as

compared to that of the single components. In addition to the total shift of the processes of nitrates decomposition to lower temperatures, the well-expressed effects of MnO_2 to Mn_2O_3

transformation within temperature range 550-600 °C are not observed, too. Probably the reason for this phenomenon is the inclusion of manganese in the more complex spinel structures.

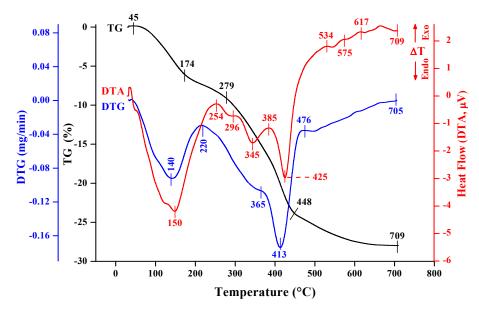


Fig. 1 Thermal analysis of La(NO₃). xH_2O/γ -Al₂O₃

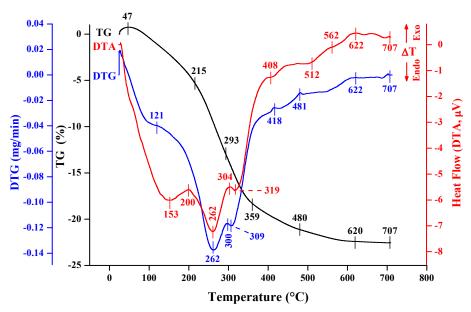


Fig. 2 Thermal analysis of $Cu-La/\gamma-Al_2O_3$ catalyst with Cu/La molar ratio 2:1

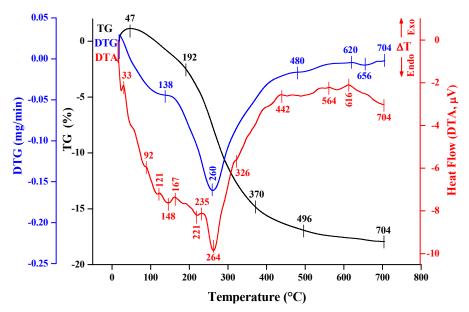


Fig. 3 Thermal analysis of Cu-Mn-La/γ-Al₂O₃ catalyst with Cu/(Mn+La) 2:1 and Mn/La molar ratio 1.5 (40% Mn replacement by La)

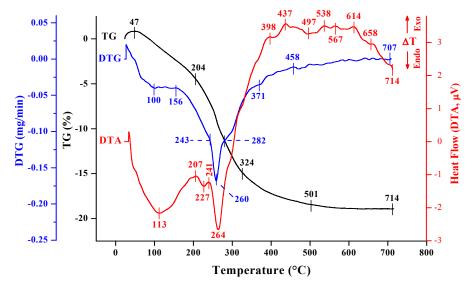


Fig. 4 Thermal analysis of Cu-Mn-La/γ-Al₂O₃ catalyst with Cu/(Mn+La) 2:1 and Mn/La molar ratio 0.67 (60% Mn replacement by La)

• Texture Measurements

In Table II are listed the results for specific surface area and pore volume of the support and mixed Cu-Mn-La/ γ -Al₂O₃ samples with Cu/(Mn+La) molar ratio 2:1 and 1:5. It is seen that the values for the specific surface of all catalysts are very similar.

The adsorption-desorption isotherm and pore size distribution of Cu/(Mn+La) 1:5 sample with molar ratio Mn/La 4.0 (20% Mn replacement by La) are presented in Fig. 5. It can be seen that the catalyst shows H1-type hysteresis loop with capillary condensation at a relative pressure $p/p_{\rm o}=0.4.$ The adsorption increases gradually with an increase in $p/p_{\rm o}$ without steep jump of the hysteresis curve. The slope and

the height of the step are a clear indication for a well-defined mesopore with a narrow pore size distribution.

TABLE II

SPECIFIC SURFACE AREA AND PORE VOLUME OF SUPPORT AND SELECTED

CATALYSTS

Composition	S_{BET} $m^2.g^{-1}$	V _{total} cm ³ .g ⁻¹
Al_2O_3	219	0.40
* Cu/(Mn+La) 1:5	218	0.29
** Cu/(Mn+La) 2:1	198	-
*** Cu/(Mn+La) 2:1	207	-

* Calcination temperature 450° C, active component loading 20° % and fraction 0.6--1.0 mm.

** Molar ratio Mn/La 4.00 (20% Mn replacement by La).

*** Molar ratio Mn/La 0.67 (60% Mn replacement by La).

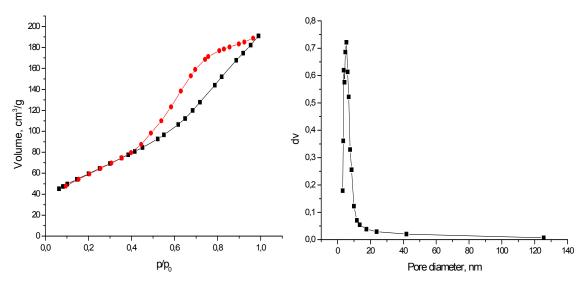


Fig. 5 Adsorption-desorption isotherm and pore size distribution of Cu/(Mn+La) 1:5 sample with molar ratio Mn/La 4.0 (20% Mn replacement by La)

• XRD

In Fig. 6 are presented the results of powder X-ray analysis of pure lanthanum catalyst and copper-manganese catalysts with molar ratio Cu/(Mn+La) 2:1 and 1:5 after complete replacement of Mn with La. In the diffractogram of the pure lanthanum catalyst are observed only the diffraction lines of γ -Al₂O₃ with a reduced intensity in comparison with the pure support. Additional lines, proving the formation of a new phase, are not registered. The diffraction patterns of Cu-La samples differ significantly. Sharp reflections at $2\theta = 35.6$, 38.8, 48.6 and 61.8° assigned to CuO phase (marked with *) are clearly identified in the diffractogram related to the Cu-La sample with ratio 2:1, while the XRD pattern of Cu/La 1:5 sample is very similar to that of La₂O₃-containing sample.

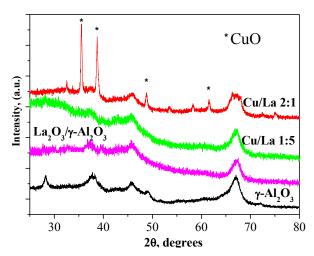


Fig. 6 XRD patterns of La and Cu-Mn-La catalysts with Cu/(Mn+La) molar ratio 2:1 and 1:5 after total replacement of Mn by lanthanum

In Fig. 7 are compared the XRD patterns of the catalyst with Cu/Mn molar ratio 2:1, in which manganese is replaced

partially or completely by lanthanum. The reflections typical for CuO dominate in all diffractograms, but their intensity slightly decreases after partial substitution of Mn by La. It is interesting to note that the highest degree of crystallinity is observed after total substitution of Mn by La.

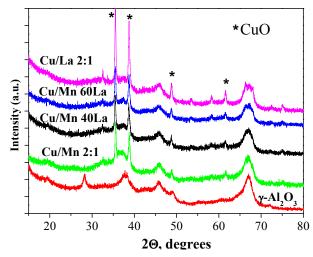


Fig. 7 XRD patterns of La and Cu-Mn-La catalysts with Cu/(Mn+La) molar ratio 2:1 after partial or total replacement of Mn by lanthanum

Looking at the XRD patterns in Figs. 6 and 7, no evidences for formation of mixed Cu-La or Cu-Mn-La structures were found. It is obvious; however, that the presence of lanthanum influences the crystal structure of the main compounds and this effect depends on their amount. This finding is in agreement with reported by He et al. results [10] that the modification with La₂O₃ of Cu-Mn oxide catalysts (atomic ratio of 1:1) improves the stability of the catalysts, the dispersity of the Cu-Mn compounds and results in a more uniform distribution. According to the same authors the lanthanum ions were not included in the $\text{Cu}_{1.5}\text{Mn}_{1.5}\text{O}_4$ spinel,

which was identified in all samples, but led to a change in the adsorption properties and catalytic behavior of the mixed samples.

TEM

The morphological characteristics of the sample Cu/(Mn+La) with molar ratio 2:1 and 60% replacement of the manganese by lanthanum were studied by TEM. Elongated crystallites of Al_2O_3 and finely dispersed spherical grains of supported components are clearly observed in Fig. 8.

The elemental mapping analysis clearly reveals that all elements supported (Cu, Mn and La) are homogeneously distributed on the support (Fig. 9).

In order to receive more detailed information about the phase composition, a selected region of the image, obtained by TEM was analyzed (Fig. 10). The distances among the fringes were measured and the spacing of the fringes 0.239, 0.2028 and 0.1569 nm closely corresponds to the (1 0 2), (1 1 0) and (2 0 2) lattice plane of La₂O₃. These results demonstrate the formation of a separate phase of La₂O₃, which is hard discernible by XRD probably due to its small amount. Additionally, in SAED pattern is demonstrated the presence of a separate phase of CuO and spinel phase Cu_{1.5}Mn_{1.5}O₄.

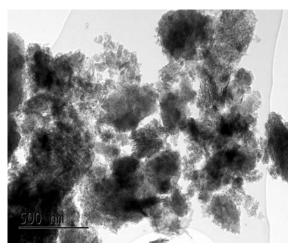


Fig. 8 TEM image of Cu-Mn-La catalysts with Cu/(Mn+La) molar ratio 2:1 (60% Mn replacement by La)

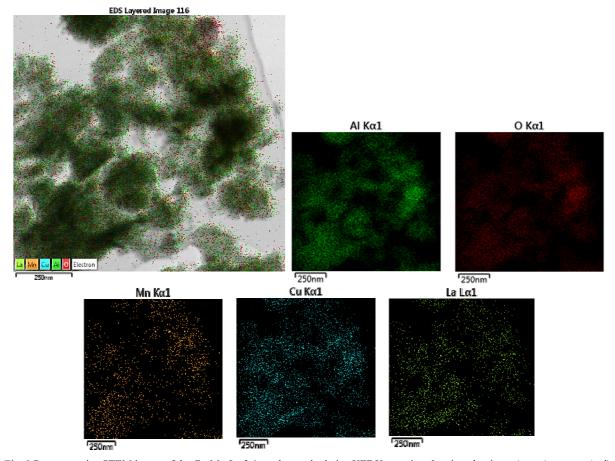


Fig. 9 Representative STEM image of the Cu-Mn-La 2:1 catalyst and relative XEDX mapping showing aluminum (green), oxygen (red), manganese (yellow), copper (blue), and lanthanum (light green) distribution

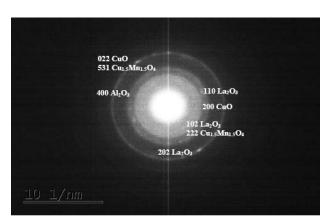


Fig. 10 Polycrystalline SAED pattern of Cu-Mn-La sample with Cu/(Mn+La) molar ratio 2:1 (60% Mn replacement by La)

• Temperature Programmed Reduction (TPR)

The study of reduction behaviour provides additional information for better interpretation of catalytic performance. The reduction profiles of the samples with a molar ratio Cu/Mn of 2:1 and 1:5, after total substitution of Mn with La, are shown in Fig. 11. The profiles of unmodified with La samples are presented for comparison. The analysis of results showed that addition of lanthanum affects negatively the reducibility. It should be noted that La₂O₃ is irreducible but its presence influences the reduction behavior of other components. A stronger effect was observed in the case of sample with molar ratio Cu/Mn 2:1. The low-temperature component with a T_{max} at 192 °C associated with the presence of highly dispersed CuO particles was shifted to a higher temperature ($T_{max} = 230$ °C) and the intensity was significantly reduced. The profile of the Cu/La 2:1 sample was complex and could be related to the presence of copper oxide particles with different size. This result is in agreement with the data from XRD analysis indicating higher crystallinity of CuO phase in the sample with total replacement of Mn with La, i.e. Cu/La 2:1.

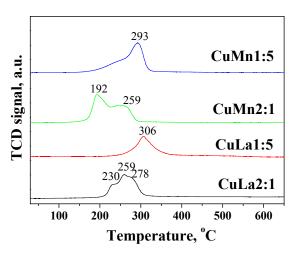


Fig. 11 TPR profiles of $Cu-Mn/\gamma-Al_2O_3$ samples with molar ratio Cu/Mn 2:1 and 1:5 and of samples with the same molar ratio and 100% replacement of Mn by La

The reducibility of CuO was also hampered in the sample with molar ratio Cu/La 1:5. In that case, the temperature peak was slightly shifted to a higher temperature. Moreover, the low-temperature shoulder in the profile of the Cu/Mn 1:5 disappeared. A symmetric peak with a maximum at 306 °C was typical for the reduction of bulk CuO. The result can be explained with the effect of La on the crystallization of the CuO and formation of particles with similar size. The reduction process $CuO \rightarrow Cu_2O \rightarrow Cu^0$ proceeded in one single step. In contrast, the presence of Mn is beneficial for formation of highly dispersed CuO particles with improved reducibility, respectively enhanced catalytic activity. The lack of a positive effect on the reduction behavior in the presence of La was confirmed by comparison of TPR profiles of the samples with molar ratio Cu/Mn 2:1, in which Mn was partially or completely replaced by La. A tendency of T_{max} shift to higher reduction temperature at increasing the content of La can be seen in Fig. 12. The opposite effect was observed in the profile of the sample with 60 % replacement of Mn by La. The probable reason should be the availability of highly dispersed Cu-containing compounds in the composition of this sample.

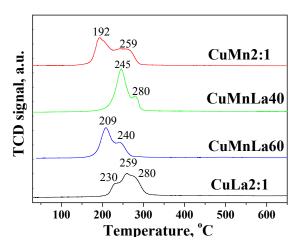


Fig. 12 TPR profiles of Cu-Mn/ γ -Al₂O₃ samples with molar ratio Cu/Mn 2:1 after partial or total replacement of Mn by La

• Activity Measurements

The results for CO, methanol and DME oxidation over Cu-Mn-La/ γ -Al₂O₃ catalyst with molar ratio Cu/(Mn+La) 2:1 and 1:5, in which Mn is replaced by La in the whole concentration range from 0 to 100%, are presented in Figs. 13-17. The results, presented in Fig. 13 indicate that the catalytic activity of the samples investigated varies significantly at the whole temperature range depending on the catalysts composition. There is a clear trend of decreased activity by increasing the content of lanthanum. The oxidation reaction started over 80°C, while overall mixed Cu-Mn-La/ γ -Al₂O₃ samples complete CO oxidation was achieved at temperatures in the range 220-240 °C. For nonmodified Cu-Mn/ γ -Al₂O₃ catalyst, this temperature was 180° C and for sample with total replacement of Mn, i.e. Cu-La/ γ -Al₂O₃ - significantly above 240°C.

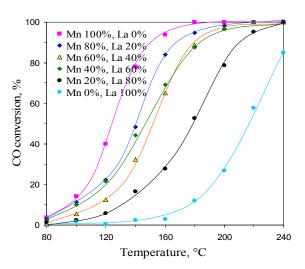


Fig. 13 Temperature dependence of CO oxidation over Cu-Mn-La/ γ -Al₂O₃ catalyst with Cu/(Mn+La) molar ratio 2:1

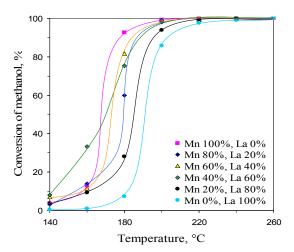


Fig. 14 Temperature dependence of CH₃OH oxidation over Cu-Mn-La/γ-Al₂O₃ catalyst with Cu/(Mn+La) molar ratio 2:1

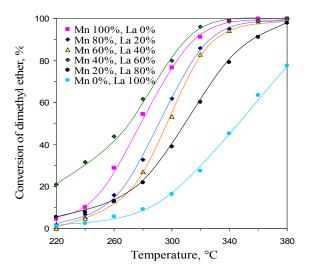


Fig. 15 Temperature dependence of DME oxidation over Cu-Mn-La/ γ -Al₂O₃ catalyst with Cu/(Mn+La) molar ratio 1:5

The oxidation of methanol (Fig. 14) over all samples started at 140 °C and complete oxidation was reached at 200-240 °C, observing the same tendency as in CO oxidation. In this case the most active again was Cu-Mn/γ-Al₂O₃ and the lowest activity indicated Cu-La/γ-Al₂O₃. The oxidation of DME (Fig. 15) began at 220 °C, and complete oxidation was attained at about 360 °C except for the samples, containing a large amount of La (Mn 20%/La 80% and La 100%). In contrast to CO and methanol oxidation, the best performance for DME oxidation was demonstrated by the sample modified with 40% La.

The trend in the CO and methanol oxidation (Figs. 16 and 17) over the samples with molar ratio Cu/(Mn+La) 1:5 is similar to those represented in Figs. 13 and 14. The samples with a high content of manganese show high catalytic activity, while $Cu-La/\gamma-Al_2O_3$ exhibit the lowest activity.

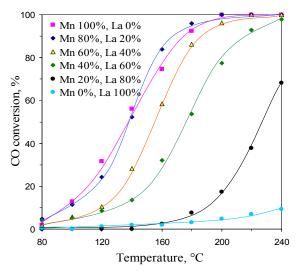


Fig. 16 Temperature dependence of CO oxidation over Cu-Mn-La/γ-Al₂O₃ catalyst with Cu/(Mn+La) molar ratio 1:5

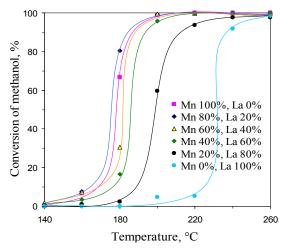


Fig. 17 Temperature dependence of CH₃OH oxidation over Cu-Mn-La/γ-Al₂O₃ catalyst with Cu/(Mn+La) molar ratio 1:5

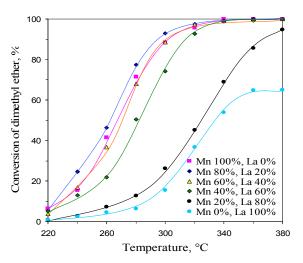


Fig. 18 Temperature dependence of DME oxidation over Cu-Mn-La/γ-Al₂O₃ catalyst with Cu/(Mn+La) molar ratio 1:5

The differences in DME oxidation (Fig. 18) over samples with molar ratio Cu/(Mn + La) 1:5 were more pronounced than those over the samples with molar ratio Cu/(Mn+La) 2:1. After a slight activity increase due to replacement of manganese by 20% La, a clear tendency of decreased DME conversion was observed with increasing of the lanthanum content.

For easier interpretation of the results and assessment of the impact of manganese substitution by lanthanum in the mixed Cu-Mn-La catalysts some data are summarized in Figs. 19 and 20.

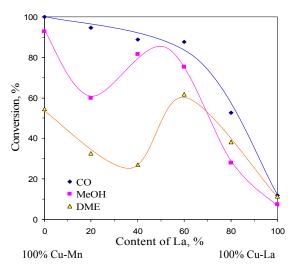


Fig. 19 Effect of lanthanum amount in the active component of Cu-Mn-La/ γ -Al $_2$ O $_3$ catalyst with a molar ratio Cu/(Mn + La) 2:1 on CO, CH $_3$ OH and DME oxidation ($T_{CO} = 180$ °C, $T_{MeOH} = 180$ °C, $T_{DME} = 280$ °C)

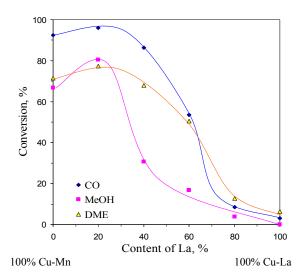


Fig. 20 Effect of lanthanum amount in the active component of Cu-Mn-La/ γ -Al₂O₃ catalyst with a molar ratio Cu/(Mn + La) 1:5 on CO, CH₃OH and DME oxidation (T_{CO} = 180 °C, T_{MeOH} = 180 °C, T_{DME} = 280 °C)

The negative role of lanthanum on the catalytic activity towards CO oxidation over both groups' catalysts is obvious. A crucial influence in this case has the activity of the individual components and lanthanum oxide acts as a structural additive. The same trend of decreased activity under increasing of the lanthanum content was observed in methanol oxidation, although there are some specific features. The catalytic activity passes through a clearly defined maximum and then decreases sharply for both groups of catalysts. The most probable reason could be formation of uniformly distributed finely dispersed particles of CuO and Cu_{1.5}Mn_{1.5}O₄ at these ratios of the components.

In contrast to the finding for higher activity in CO and methanol oxidation over the samples with molar ratio Cu/(Mn+La) 2:1 in comparison with the samples with molar ratio Cu/(Mn+La) 1:5, the performance for the DME oxidation is opposite. The explanation for these experimental results is the higher activity of copper-rich samples with respect to CO and methanol oxidation, and the higher activity of manganese-rich samples in respect to DME oxidation. The replacement of 20% of manganese by lanthanum in the manganese-rich samples leads to increased activity in DME and methanol oxidation. The catalytic activity in the CO, methanol and DME oxidation could not be explained by the influence of the specific surface area which changes in a very narrow range among different samples (Table II). Obviously, the catalysts composition plays a decisive role in the oxidation processes.

IV. CONCLUSIONS

The results presented showed that:

The substitution of manganese by lanthanum in the mixed Cu-Mn-La/γ-Al₂O₃ catalyst with molar ratio Cu/(Mn + La) 1:5 up to 20% results in increased catalytic activity in CO, CH₃OH and DME oxidation. Expected better

stability in the presence of lanthanum makes these samples interesting from a practical point of view. The samples with molar ratio Cu/(Mn+La) 2:1 and replacement of manganese by lanthanum in the entire concentration range exhibited decreased oxidation activity in respect of the three compounds under investigation.

The active component of mixed Cu-Mn-La/γ-Al₂O₃ catalysts contains at least four compounds depending on the molar ratio Cu/Mn/La - CuO, La₂O₃, MnO₂ and Cu_{1.5}Mn_{1.5}O₄. The reducibility of the samples and the correlation with catalytic activity allowed to suppose the formation of finely dispersed copper-containing structures with increased activity in appropriate ratio between the starting components.

ACKNOWLEDGMENT

Authors gratefully acknowledge the financial support by the National Science Fund (Project DFNI T 02/4).

REFERENCES

- Y. Nishihata, J. Mizuki, T. Akao, H. Tanaka, M. Uenishi, M. Kimura, N. Hamada, "Self-regeneration of a Pd-perovskite catalyst for automotive emissions control", *Nature*, 418 (6894), pp. 164-167 2002.
- [2] H. Tanaka, M. Misono, "Advances in designing perovskite catalysts", Current Opinion in Solid State and Materials Science, 5 (5), pp. 381-387, 2001.
- [3] M. Stoyanova, P. Konova, P. Nikolov, A. Naydenov, St. Christoskova, D. Mehandjiev "Alumina-supported nickel oxide for ozone decomposition and catalytic ozonation of CO and VOCs", Chemical Engineering Journal 122 (1-2), pp 41-46, 2006.
- [4] S. Moreau, J. Choisnet, F. Beguin, J., "Development of La_xMO_y nanoparticles dispersed in a layered silicate matrix", *Phys. Chem. Solids*, 57, pp. 1049-1056, 1996.
- [5] E. A. Lombardo, M.A. Ulla, "Perovskite oxides in catalysis: Past, present and future", *Res. Chem. Intermed.*, 24 (5), pp. 581-592, 1998.
 [6] X. Chen, S.A.C. Carabineiro, P.B. Tavares, J.J.M. Orfao, M.F.R.
- [6] X. Chen, S.A.C. Carabineiro, P.B. Tavares, J.J.M. Orfao, M.F.R. Pereira, J.L. Figueired, "Catalytic oxidation of ethyl acetate over La-Co and La-Cu oxides", J. Envir. Chem. Eng., 2, pp. 344-355, 2014.
- [7] R. Prasad, P. Singh, "A Review on CO oxidation over copper chromite catalyst", Catal. Rev.: Sci. Eng., 54, pp. 224–279, 2012.
- [8] A. Urbutis, S. Kitrys, "Structure and activity of CuO catalysts promoted with CeO₂ and La₂O₃ for complete oxidation of VOCs", *Chemija.*, 24 (2), pp. 111–117, 2013.
- [9] S. Mentus, D. Jeli, V. Grudi, "Lanthanum nitrate decomposition by both temperature programmed heating and citrate gel combustion. Comparative study", J. Therm. Anal. Calorim., 90 (2), pp.393–39, 2007.
- [10] H.E. Runxia, H. Jiang, W.U. Fang, K. Zhi, N. Wang, C. Zhou, Q. Liu, "Effect of doping rare earth oxide on performance of copper-manganese catalysts for water-gas shift reaction", J. Rare Earths, 32 (4), pp. 298-305, 2014.